

## Standard Model Measurements

Philip C. Harris on behalf of the CMS collaboration  
*Laboratory of Nuclear Science, Massachusetts Institute of Technology, Cambridge, Ma, USA*



We present several measurements in the domain of electroweak and top physics in proton-proton collisions at the LHC using a centre-of-mass energy of 7 TeV. Data was collected with the CMS experiment during the year 2010, amounting to a total integrated luminosity of 36 pb<sup>-1</sup>. All measurements are compared with theory and found to be consistent with standard model predictions.

### 1 Introduction

In 2010 CMS<sup>1</sup> running, a total of 47 pb<sup>-1</sup> integrated luminosity was delivered and 43 pb<sup>-1</sup> of that was recorded to tape. This yields 36 pb<sup>-1</sup> of certified good data at  $\sqrt{s} = 7$  TeV. This data resulted in a prodigious amount of W, Z, and top based measurements. These measurements consist of processes with cross sections ranging over three orders of magnitude from  $\approx 10$  nb to  $\approx 10$  pb. The precision of these measurements ranged inversely from 1% for processes with a large cross section upwards to 30% for processes with a small cross section.

Standard model measurements serve as a foundation to understanding new physics. Moreover, due to their large cross sections, W and Z boson related measurements are a powerful tool to constrain QCD calculations at 7 TeV and further improve understanding of quark and gluon parton distribution functions. Top quark pair production is the highest energy standard model resonant process. Thus measurements of top quark properties provide a tool to study high energy measurements at the LHC.

In most cases, the measurements presented here are the first measurements of its kind at 7 TeV. In the case of the top quark, this is the first time the top quark has been studied outside of the Tevatron.

In the following document, the CMS results of the 2010 LHC data concerning electroweak and top measurements are presented. These consist of: the W and Z total and differential cross sections, various diboson observations, the top pair production and single production cross sections, and additional studies of the top quark.

## 2 Selection and Calibration of the CMS detector

In order to perform all of the presented measurements, each event was required to have at least one isolated high  $p_T$  electron or muon in the final state. With the exception of the di-lepton  $t\bar{t}$  analysis, the leptons in all of these events were required to fire the lowest energy unrescaled single electron or single muon trigger. For muon analyses, this requirement allowed for a single muon with  $p_T > 15$  GeV/c. For the electron, the trigger requirements evolved with increasing luminosity, starting with a 10 GeV photon trigger and ending at an electron trigger with  $E_T > 22$  GeV/c and loose electron shower shape requirements. The di-lepton  $t\bar{t}$  cross section analyses additionally allowed events which had passed a di-electron trigger.

Following the trigger requirement, leptons were required to pass identification cuts yielding a well reconstructed lepton originating from the primary vertex. In order to avoid selection of leptons from hadronic decays, leptons were additionally required to be isolated by removing events with large energy deposits within a cone in  $\eta$  and  $\phi$  along the path of the lepton.

The efficiency of the triggers, identification and isolation cuts on leptons utilize the “tag and probe” method on Z boson leptonic decays. In this method, a Z boson event is “tagged” by requiring a well reconstructed, isolated lepton along with a component of the second lepton (*i.e. track in the tracker*), which when combined have a mass compatible with the Z boson. The tagged event is then used to “probe” for an additional component of the second lepton (*i.e. track in the muon chambers*). This efficiency measurement in data is compared with that of Monte-Carlo simulation to determine a set of correction factors that translate efficiency measurements to other kinematic regimes.

The lepton energy resolution, and missing transverse energy ( $\cancel{E}_T$ ) modelling are also quantified by utilizing Z events. In the case of the  $\cancel{E}_T$ , which is defined as the negative vector sum of all of the deposits in the detector, calibration was performed by comparing the lepton measured Z boson  $p_T$  with the measured Z boson  $p_T$  from the rest of the detector. The lepton energy resolution is determined by fitting the Z mass as a function of the two leptons’ ( $\eta, \phi$ ) coordinates.

In some analyses, additional selections on a jet or a b-tagged jet are performed. To calibrate the reconstructed jet energy and resolution, jets originating in di-jet and  $\gamma$ +jet events are balanced with its opposite component. This balance is further compared with simulation yielding a set of uncertainties and corrections on the simulated jets. B-tagged jets are studied by tagging semileptonic b-decays in jet events and looking at the performance of the b-tag identification.

## 3 Electroweak Analyses

### 3.1 W/Z Inclusive cross section

The W/Z and inclusive sections have been previously measured with  $2.7$  pb $^{-1}$  or data <sup>2</sup>, in this conference an updated result with the full 2010 dataset is presented <sup>3</sup>. The inclusive Z cross section measurement is performed by requiring two well isolated leptons with a combined mass  $m_{\ell\ell}$  given by  $60 < m_{\ell\ell} < 120$  GeV/c<sup>2</sup>. The cross section is then determined by fitting the data with a simulated template of the Z mass lineshape where energy scale and, resolution corrections have been applied. The W boson inclusive cross section is determined by requiring single isolated leptons and fitting the  $\cancel{E}_T$  with a  $\cancel{E}_T$  template correct to reflect the W boson  $\cancel{E}_T$  in data.

The results of the cross section measurements and the cross section ratios are shown in table 1. The final results are, in most cases, strongly limited by the theoretical and luminosity uncertainties. These put a set of tight constraints on theoretical predictions.

Table 1: W and Z boson cross section and ratios

Measurement	Value $\pm(stat) \pm(sys) \pm(theory) \pm(lumi)$	Theory <sup>[<math>\beta</math>]</sup>
$\sigma(W) \times BF(W \rightarrow \ell\nu)$ pb	$10\,31 \pm 0\,02 \pm 0\,09 \pm 0\,10 \pm 0\,41$	$10\,44 \pm 0\,52$
$\sigma(W^+) \times BF(W^+ \rightarrow \ell^+\nu)$ pb	$6\,04 \pm 0\,02 \pm 0\,06 \pm 0\,08 \pm 0\,24$	$6\,15 \pm 0\,29$
$\sigma(W^-) \times BF(W^- \rightarrow \ell^-\nu)$ pb	$4\,26 \pm 0\,01 \pm 0\,04 \pm 0\,07 \pm 0\,17$	$4\,29 \pm 0\,23$
$\sigma(Z) \times BF(Z \rightarrow \ell^+\ell^-)$ pb	$0\,975 \pm 0\,007 \pm 0\,007 \pm 0\,018 \pm 0\,039$	$0\,97 \pm 0\,04$
$\sigma(W) \times BF$ $\sigma(Z) \times BF$	$10\,54 \pm 0\,07 \pm 0\,08 \pm 0\,16$	$10\,74 \pm 0\,04$
$\sigma(W^+) \sigma(W^-)$	$1\,421 \pm 0\,006 \pm 0\,014 \pm 0\,030$	$1\,43 \pm 0\,04$

### 3.2 W Polarization measurement

In a proton-proton collider, W bosons produced at a transverse momentum  $> 50$  GeV  $c$  are typically produced with a gluon jet, which may induce a polarization in the W boson. Due to the CP asymmetry of the initial state, production of a left handed W boson is favored at high  $p_T$ . This effect is only true for proton-proton colliders where the CP conjugate is not present<sup>4</sup>.

To measure the W polarization, a fit is performed to the transverse projection of the lepton boson direction for Ws with  $p_T > 50$  GeV. The variable that is fit, is known as the LP variable and is defined to be

$$LP = \frac{\vec{p}_T(\ell) \cdot \vec{p}_T(W)}{p_T(W)^2} \quad (1)$$

Where in this case  $\vec{p}_T(\ell)$  and  $\vec{p}_T(W)$  are the transverse momentum of the lepton and the W boson respectively. The fit yields both the left-right asymmetry and the longitudinal polarization of the  $W^+$  and  $W^-$ . The measured left right asymmetry of  $0\,300 \pm 0\,031(stat) \pm 0\,034(sys)$  for  $W^+$  and  $0\,226 \pm 0\,031 \pm 0\,050$  for  $W^-$  bosons confirms left-handed W polarization in proton-proton colliders. The longitudinal polarization is found to be  $0\,162 \pm 0\,078(stat) \pm 0\,136(sys)$  for  $W^-$  bosons and  $0\,192 \pm 0\,075(stat) \pm 0\,089(sys)$  for  $W^+$  bosons.

### 3.3 Di-Lepton differential cross sections

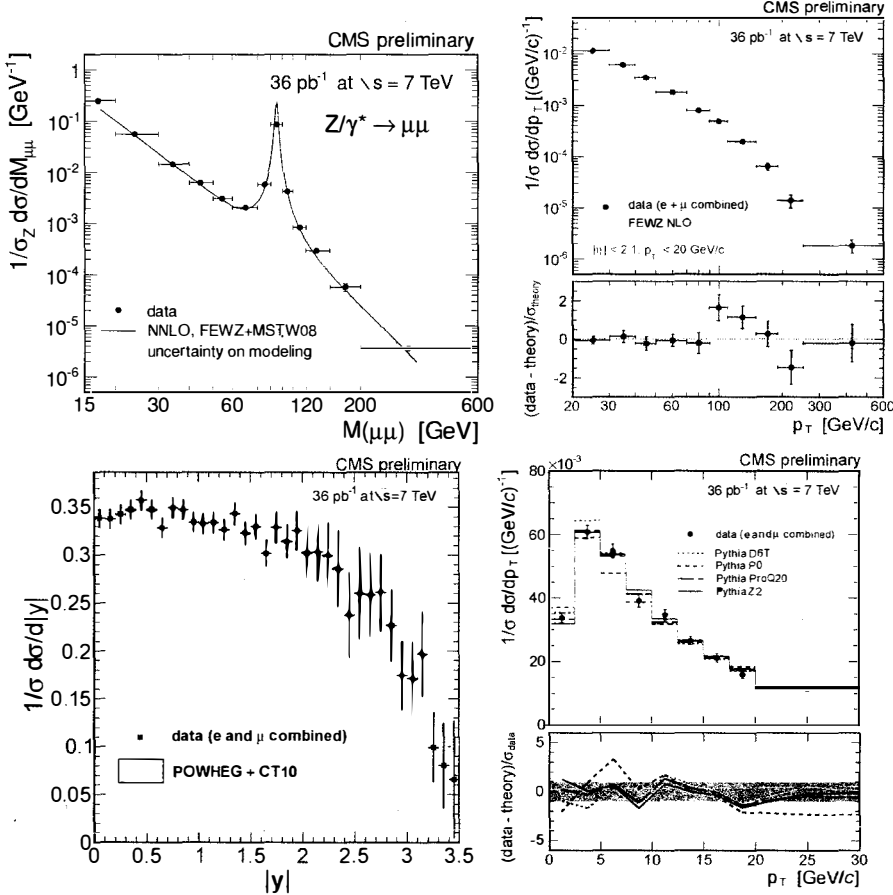
In addition to the inclusive Z production cross section, differential production for the Z boson  $y, p_T$ <sup>5</sup>, and  $mass(m_{\ell\ell})$  distributions<sup>6</sup> are also measured. In all of these distributions, the background subtracted, per-bin yield is calculated and then the distribution is unfolded to the differential distribution before final state radiation (FSR) correction.

The differential distributions are shown in figure 1. The  $y$  and  $p_T$  distributions are measured for di-lepton events within a mass window of  $60 < m_{\ell\ell} < 120$  GeV/ $c^2$ . The resulting rapidity distribution goes out to a rapidity of  $y < 3.5$ . The rapidity measurement beyond  $y > 2.4$  is performed with the electron reconstruction in the forward calorimeter (reconstruction out to  $\eta < 4$ ). The measured distribution is sensitive to the the quark parton distributions. Following figure 1, the data favors well the prediction obtained with the CTEQ10 pdf set. The  $p_T$  distribution is sensitive to both higher order matrix element corrections and resummation. At low  $p_T$  the best matching calculation results from the Pythia Pro Q20 tune<sup>7</sup>. At high  $p_T$  the NLO calculation is sufficient to describe the data up to a region of 200 GeV/ $c$ . The mass differential distribution  $m_{\ell\ell}$  matches the NNLO calculation as performed by FEWZ<sup>8</sup>.

### 3.4 W+Jets and Z+Jets cross sections

The W and Z jet multiplicity and its trend from small jet multiplicities to large jet multiplicities are powerful tests of standard model QCD calculations. The measurement is performed by

Figure 1: Di-Lepton differential distributions for  $m_{\ell\ell}$  in muons (top left),  $p_T$  for electrons and muons combined where  $p_T < 30$  GeV/c (top right) and where  $p_T > 20$  GeV/c (bottom right), and  $y$  for electrons and muons combined (bottom left)



counting jets with an  $E_T > 30$  GeV/c for a single and double lepton selection<sup>9</sup>. At high jet multiplicity, the single lepton +  $\cancel{E}_T$  selection has large contributions from both  $t\bar{t}$  and W boson events. Consequently, the W boson cross section for the specified jet multiplicity bin is extracted from a 2-dimensional fit in the variables transverse mass and number of b-tags. The final jet multiplicity is unfolded to the particle level incorporating energy scale and mis-modelling uncertainties.

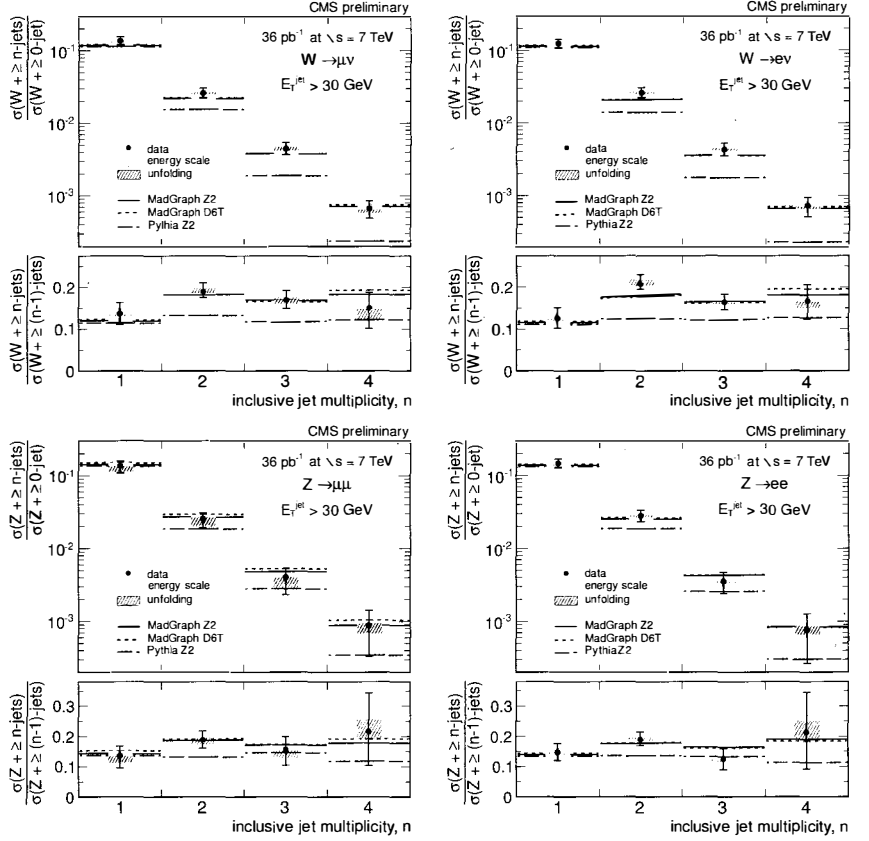
The W and Z jet multiplicities are shown in figure 2. The resulting W and Z jet multiplicities demonstrate the effectiveness of MLM Monte-Carlo simulation<sup>10</sup>. This is indicated by the data simulation agreement in jet multiplicity of Madgraph and not Pythia. The per-jet cross section follows a trend given by (for n-jets)

$$\frac{\sigma_{n+1}}{\sigma_n} = \alpha + \beta n \quad (2)$$

This trend, known as the Berends-Giele scaling<sup>11</sup> can be fit for to obtain an overall prediction

of jet production. The resulting values for  $\alpha$  and  $\beta$  are shown in table 2. The values for  $\alpha$  in W production are smaller than the predicted standard model value indicating a slightly larger cross section in the high jet multiplicity bins.

Figure 2: W and Z Jet multiplicity measurements for W bosons (top), and Z bosons(bottom) separated out by muons(left), and electrons(right)



### 3.5 Z+b Jet production

In addition to Z+Jet measurements, a measurement of the b-jet production was performed in CMS by requiring Z events with 1 jet having a  $p_T > 25\text{GeV}/c$  and a high purity b-tag on the jet<sup>12</sup>. The results presented in table 2 are in close agreement with NLO theory predictions.

### 3.6 Z+ $\gamma$ production

In addition to single boson measurements, several di-boson measurements have been performed on the first  $36\text{pb}^{-1}$  of data. One such measurement is the measurement of a photon with  $p_T > 10\text{GeV}/c$  in association with a Z boson<sup>13</sup>. In order to separate out photon production from radiative photons from the lepton final state radiation, the photon is required to be a distance  $\Delta R = \sqrt{\Delta\eta^2 + \Delta\phi^2} > 0.7$  from any lepton in the Z +  $\gamma$  event. The resulting events

Table 2: Properties of Z + jets and W + jets

Measurement	Value( $\pm(stat) \pm(sys)$ )	Theory(Madgraph)
$\alpha(Z \rightarrow \mu^+\mu^-)$	$5.8 \pm 1.2 \pm 0.6$	$4.8 \pm 0.1$
$\beta(Z \rightarrow \mu^+\mu^-)$	$-0.2 \pm 1.0 \pm 0.3$	$0.4 \pm 0.1$
$\alpha(Z \rightarrow e^+e^-)$	$5.0 \pm 1.0 \pm 0.1$	$5.0 \pm 0.1$
$\beta(Z \rightarrow e^+e^-)$	$0.7 \pm 0.8^{+0.3}_{-0.6}$	$0.5 \pm 0.1$
$\alpha(W \rightarrow \mu\nu)$	$4.3 \pm 0.3 \pm 0.3$	$5.2 \pm 0.1$
$\beta(W \rightarrow \mu\nu)$	$0.7 \pm 0.3 \pm 0.5$	$0.2 \pm 0.1$
$\alpha(W \rightarrow e\nu)$	$4.6 \pm 0.4^{+0.2}_{-0.0}$	$5.2 \pm 0.1$
$\beta(W \rightarrow e\nu)$	$0.5 \pm 0.4^{+0.2}_{-0.1}$	$0.4 \pm 0.1$
$\sigma(Z \rightarrow \mu^+\mu^- + b)$ $\sigma(Z \rightarrow \mu^+\mu^- + j)$	$0.054 \pm 0.010 \pm 0.012$	$0.043 \pm 0.005$
$\sigma(Z \rightarrow e^+e^- + b)$ $\sigma(Z \rightarrow e^+e^- + j)$	$0.046 \pm 0.008 \pm 0.011$	$0.047 \pm 0.005$

yield a cross section measurement of  $9.4 \pm 1.0(sys) \pm 0.6(stat) \pm 0.4(lumi)$  pb in accordance with the standard model prediction of  $9.6 \pm 0.4$  pb.

## 4 Top Analyses

In this section we present all measurements performed with a top quark in the final state. Top quarks decay into a W boson and bottom quark. For  $t\bar{t}$  production, identification of one of the W bosons is performed with an isolated lepton. The second W boson is measured through either its hadronic or leptonic decay. The presence of b-tagged jets further improves the purity of the selected dataset.

### 4.1 $t\bar{t}$ Cross Section In The Di-Lepton channel

The di-lepton cross section measurement is performed by requiring two isolated leptons and the presence of large  $\cancel{E}_T$ <sup>14</sup>. To maximize separation with background the analysis is performed in jet multiplicity bins, where in each jet bin a separate  $\cancel{E}_T$  selection and background estimation from Drell-Yan and QCD contributions is performed. Uncertainties result from the lepton reconstruction and resolution, as well as the b-tag efficiency and modelling of the signal shape. The result of this method can be found in figure 3. The result compares well with the NLO and partial NNLO prediction.

### 4.2 $t\bar{t}$ Cross Section In The Lepton+Jets Channel

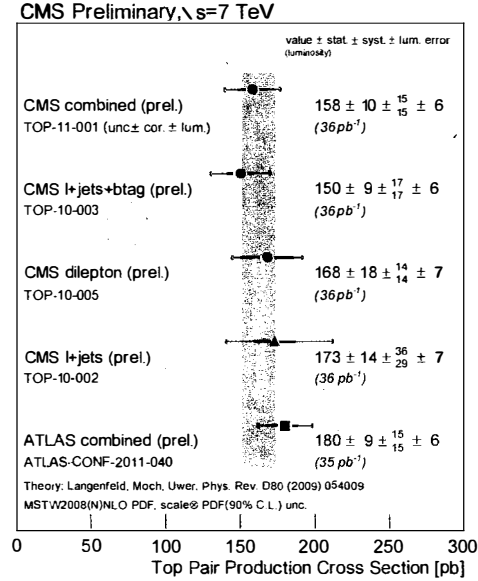
The single lepton top quark cross section is performed through two methods by requiring a single high  $p_T$  lepton and either  $\geq 3$  jets<sup>15</sup> or the presence of a b-tag<sup>16</sup>. In the instance where there is a b-tag, the yield is determined by fitting in three dimensions the vertex mass distribution of the b-tagged jet, the jet multiplicity and the number of b-tagged jets. The fit simultaneously floats the jet energy scale, the b-tag efficiency, and the W+jets  $Q^2$  scale so as to reduce the systematic uncertainty. The choice of fitting the three variables separately disentangles the signal along with the individual backgrounds coming from W+light quark flavor, W+ heavy quark flavor production, and QCD. This method is additionally performed simultaneously in lepton flavor (e and  $\mu$ ).

The method where 3 or more jets are utilized is performed by simultaneously fitting the  $\cancel{E}_T$  and the mass of the 3 jets. The fit is performed in both the electron and muon plus jets channel while separately floating the single top, W, Z, electron QCD and muon QCD contributions. The measurement parallels the cross section measurement where a b-tag is applied. Deviations in

this lepton+jets cross section measurement with the b-tagged measurement may indicate new physics.

The resulting combined cross section<sup>17</sup> from the two different channels (excluding the non b-tagged cross section) is  $\sigma = 158 \pm 10(stat) \pm 15(sys) \pm 6(lumi)pb$ . This value is within the uncertainty band of the NLO cross section, with an uncertainty comparable to that of the uncertainty on the partial NNLO cross section prediction. A comparison of the three cross section measurements is shown in figure 3, all three measurements are in close agreement amongst themselves and the predicted measurement.

Figure 3: Summary of various inclusive  $t\bar{t}$  production cross sections. The inner error bars of the data points correspond to the statistical uncertainty. The thin error bars incorporate the systematic uncertainties and the brackets incorporate the luminosity uncertainty



### 4.3 Top Quark Mass Measurement

The top quark mass measurement is performed in the di-lepton channel with two different techniques<sup>18</sup>. One technique relies on an assumption on the momentum distribution of the  $t\bar{t}$  system along the beam axis. The other technique scans over the mass assumptions choosing the most likely mass assumption in accordance with lepton  $p_T$  distributions.

The resulting mass distributions from each technique are used to determine the top quark mass, which is found to be  $m_t = 175.5 \pm 4.6(stat) \pm 4.6(sys) GeV/c^2$ . This measurement is in excellent agreement with both CDF and D0 measurements of the top quark mass.

### 4.4 Single Top Cross Section Measurement

The single top cross section measurement in the t-channel was performed using both a multivariate and a fitting technique<sup>19</sup>. In each case, a selection requiring an isolated lepton, at least one b-tag, and an additional jet is applied. In the fitting method, a selection explicitly requiring no more than one b-tag is additionally applied. The fitting method was performed by fitting

in two dimensions, the observable  $\cos(\theta_{\ell_j})$ , where  $\theta_{\ell_j}$  is the angle between the lepton and the non-b-tagged jet, and the pseudorapidity of the non b-tagged jet  $\eta_j$ . The multivariate analysis incorporated a boosted decision tree of 37 observables. The resulting output variable was fitted with templates.

The results are combined taking in the correlations. The final cross section measurement,  $83.6 \pm 29.8(stat + sys) \pm 3.3(lumi)$ , is consistent with the standard model prediction of  $\sigma_{th} = 62.3^{+2.3}_{-2.4}$  pb. This is the first time the single top cross section measurement was performed without a multivariate analysis.

#### 4.5 Top Charge Asymmetry Measurement

In light of the most recent measurements from the Tevatron reporting an excess in the top quark forward-backward asymmetry<sup>20</sup> ( $A_{FB} = 0.193 \pm 0.065(stat) \pm 0.024(sys)$ ), a measurement of the top quark charge asymmetry was performed by measuring the charge asymmetry of the top  $\eta$  observable,  $\rho = \eta_t - \eta_{\bar{t}}$ <sup>21</sup>. The asymmetry is defined through the formula.

$$A_C = \frac{\rho_+ - \rho_-}{\rho_+ + \rho_-} \quad (3)$$

where  $\rho_+$  designates the sign of the  $\rho$  variable. The measurement was performed on the same selection as used in the non b-tagged lepton+jets  $t\bar{t}$  cross section analysis and then unfolded to the particle level. The measured value is found to be  $A_C = 0.060 \pm 0.134(stat) \pm 0.028^{+0.028}_{-0.025}(sys)$ , which is consistent with the standard model prediction  $A_C = 0.011$ .

## 5 Conclusions

In 2010, CMS has completed a large number of standard model measurements, which incorporate either electroweak bosons or top quarks. These measurements have all been found to be consistent with the standard model and in some cases these measurements have provided new constraints on standard model calculations, such as parton distribution functions, standard model couplings and NNLO differential calculations. In the course of these measurements a number of new techniques were developed, these techniques and further measurements will play a crucial role in the following years of LHC running.

## References

1. CMS Collaboration, “The CMS experiment at the CERN LHC”, JINST 3:S08004,2008.
2. CMS Collaboration, “Measurements of Inclusive W and Z Cross Sections in pp Collisions at  $\sqrt{s} = 7$  TeV”, JHEP 01(2011)080
3. CMS Collaboration, “Study of W and Z boson Production at  $\sqrt{s} = 7$  TeV”, *CMS PAS EWK-10-005* (2011)
4. CMS Collaboration, “First Measurement of the Polarization of W Bosons with Large Transverse Momentum in W +Jets Events at a pp Collider”, *CMS PAS EWK-10-014* (2011)
5. CMS Collaboration, “Differential Cross Section of Z boson”, *CMS PAS EWK-10-010* (2011)
6. CMS Collaboration, “Measurement of the Drell-Yan cross section ( $d\sigma/dM$ )”, *CMS PAS EWK-10-007* (2011)
7. A. Buckley, H. Hoeth, H. Lacker et al. “Systematic event generator tuning for the LHC”, Eur. Phys. J. C65 (2010) 331-357
8. K. Melnikov and F. Petriello, “The W boson production cross section at the LHC through  $O(\alpha_s^2)$ ”, Phys. Rev. Lett. 96 (2006) 231803



9. CMS Collaboration, “Rates of Jets Produced in Association with W and Z Bosons”, *CMS PAS EWK-10-012* (2011)
10. F. Maltoni and T. Stelzer, “MadEvent: Automatic event generation with MadGraph”, *JHEP* 02 (2003) 027
11. F. A. Berends, W. T. Giele, H. Kuijf et al., “Multi-jet production in W, Z events at p anti-p colliders”, *Phys. Lett. B* 224 (1989) 237.
12. CMS Collaboration, “Observation of  $Z+b$ ,  $Z\rightarrow ee, \mu\mu$  with CMS at  $\sqrt{s} = 7$  TeV”, *CMS PAS EWK-10-015* (2011)
13. CMS Collaboration, “Measurement of  $W\gamma$  and  $Z\gamma$  production in pp collisions at  $\sqrt{s} = 7$  TeV”, *CMS PAS EWK-10-008* (2011)
14. CMS Collaboration, “Measurement of the top-quark pair-production cross section in the dilepton channel at 7 TeV at  $\sqrt{s} = 7$  TeV”, *CMS PAS TOP-10-005* (2011)
15. CMS Collaboration, “Measurement of the  $t\bar{t}$  Pair Production Cross Section at  $\sqrt{s} = 7$  TeV using the Kinematic Properties of Lepton + Jet Events”, *CMS PAS TOP-10-002* (2011)
16. CMS Collaboration, “Measurement of the  $t\bar{t}$  Pair Production Cross Section at  $\sqrt{s} = 7$  TeV using  $b$ -quark Jet Identification Techniques in Lepton + Jet Events”, *CMS PAS TOP-10-003* (2011)
17. CMS Collaboration, “Combination of top pair production cross sections in pp collisions at  $\sqrt{s} = 7$  TeV and comparisons with theory”, *CMS PAS TOP-11-001* (2011)
18. CMS Collaboration, “First measurement of the the top-quark mass in the dilepton channel in pp collisions at  $\sqrt{s} = 7$  TeV”, *CMS PAS TOP-10-006* (2011)
19. CMS Collaboration, “Measurement of single top t-channel cross section in pp collisions at  $\sqrt{s} = 7$  TeV”, *CMS PAS TOP-10-008* (2011)
20. CDF Collaboration, “Measurement of the Forward-Backward Asymmetry in Top Pair Production in 3.2/fb of ppbar collisions at  $\sqrt{s} = 1.96$  TeV”, Conf. Note 9724 (March 2009)
21. CMS Collaboration, “Measurement of the charge asymmetry in top quark pair production with the CMS experiment”, *CMS PAS TOP-10-010* (2011)

